

60015 PRISTINE CATACLASTIC ANORTHOSITE, GLASS-COATED 5574 g

INTRODUCTION: 60015 is a coherent, very light gray, shock-melted and cataclastic anorthosite which is probably chemically pristine. It is largely coated with a vesicular glass up to 1 cm thick (Fig. 1). The glass contains a few white inclusions and the glass-anorthosite contact is macroscopically sharp.

60015 was probably collected about 30 m west-northwest of the Lunar Module but details of its collection, situation, and orientation are not known. It is blocky with rare fractures. Zap pits are common on two surfaces with a few on the others.

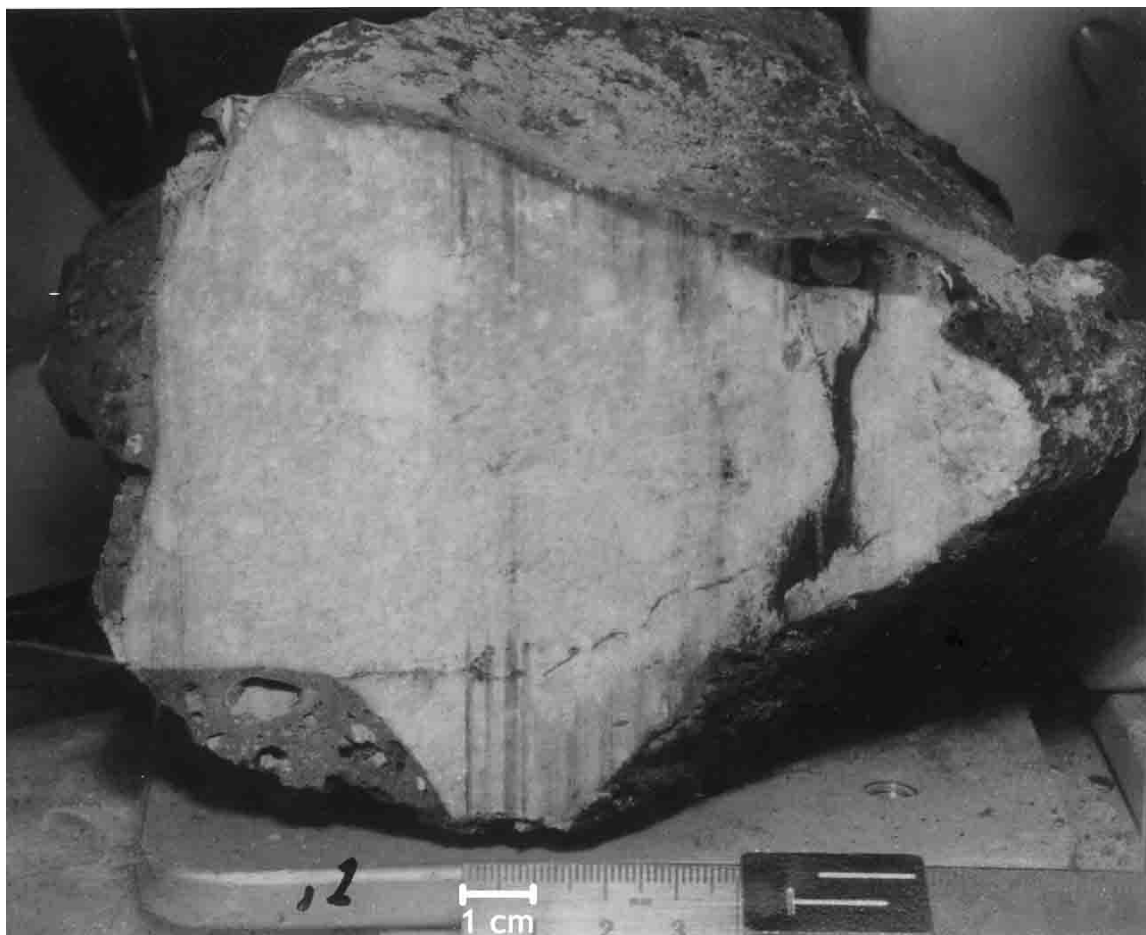


FIGURE 1.

PETROLOGY: Petrographic descriptions are given by Sclar et al. (1973), Sclar and Bauer (1974), Dixon and Papike (1975) and Juan et al. (1974). All note the brecciation and intense shock damage to the anorthosite (Fig. 2) which took place prior to the

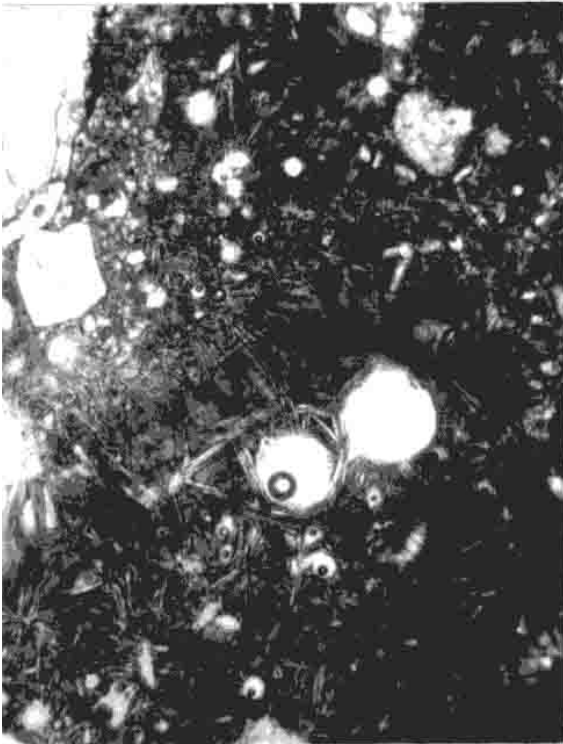
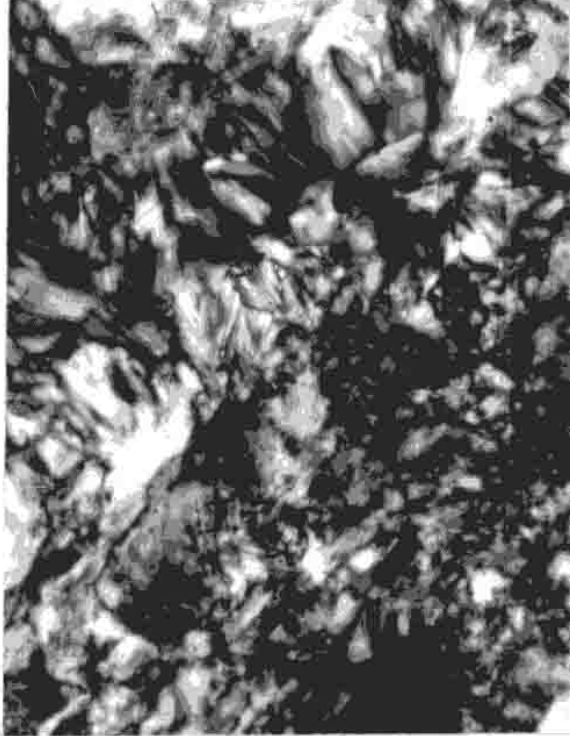


FIGURE 2. 60015,120.  
a) anorthosite, xpl. width 2mm.  
b) columnades in anorthosite, xpl. width 0.5mm  
c) glass coat, ppl. width 2mm.

emplacement of the glass coat. The anorthosite consists of more than 98% plagioclase ( $An_{95-98}$ ) with 1-2% orthopyroxene ( $En_{63}$ ) and augite (Fig. 3). Ishii et al. (1976) calculate an equilibration temperature of 987°C from the augite-orthopyroxene data of Dixon and Papike (1975). Olivine is absent, but ilmenite, Cr-spinel, troilite and minor Fe-metal are present (Dixon and Papike, 1975).

There is a bimodal grain size with grains of plagioclase 1-3 mm in diameter set in a finer-grained matrix. Plagioclases are strained with undulose and patchy extinction and some well-developed sets of shock lamellae exist. Maskelynite is not present. The intergranular areas include columnar, feathery plagioclases (Fig. 2) interpreted as resulting from a rapidly cooled intergranular shock melt. No intergranular movement took place during the shock event and temperatures are believed to have risen to over 1500°C. The progenitor was possibly porous (Sclar and Bauer, 1974). Fe-metal in the anorthosite contains little Co or Ni (Fig. 4) (Hewins and Goldstein, 1975a; Sclar and Bauer, 1974; Mao and Bell, 1976). The lowest values, which occur in the feathery plagioclase regions may be the result of shock reduction of  $Fe^{2+}$  plagioclase (Sclar and Bauer, 1974).

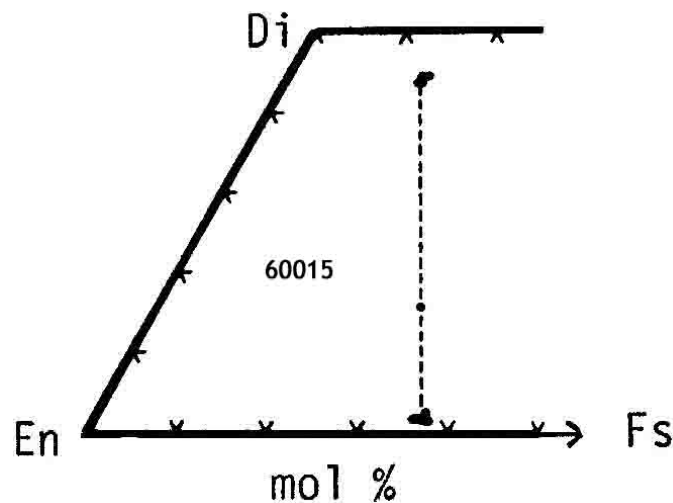


FIGURE 3. Pyroxenes; from Dixon and Papike (1975).

The glass coat is brown, vesicular and partly crystallized into skeletal microlites of plagioclase. The plagioclase-rich xenoliths and xenocrysts in the glass show no evidence of reaction with the glass, which is similar in composition to Apollo 16 soils (Table 2). Metal in the glass contains up to 30% Ni, in the meteoritic range (Fig. 4) (Hewins and Goldstein, 1975a; Mao and Bell, 1976). Mao and Bell (1976) show that metals are altered from their original meteoritic composition by reaction with the anorthosite, and that the higher Ni contents occur in metals associated with troilite and schreibersite.

The contact relationships of glass coat and anorthosite are described in detail by Sclar and Bauer (1974). The peripheral 6 mm of anorthosite lacks feathery plagioclase, but a 200

$\mu\text{m}$  boundary layer of pure, columnar plagioclase exists, and is interpreted as quenched liquid derived by melting the surface of the anorthosite. Two distinct liquids, one the anorthosite surface, the other the glass coat, existed momentarily. The heat to melt the anorthosite surface must have been mainly from the shock event which produced the glass coat, not from the glass coat itself (Sclar and Bauer, 1974).

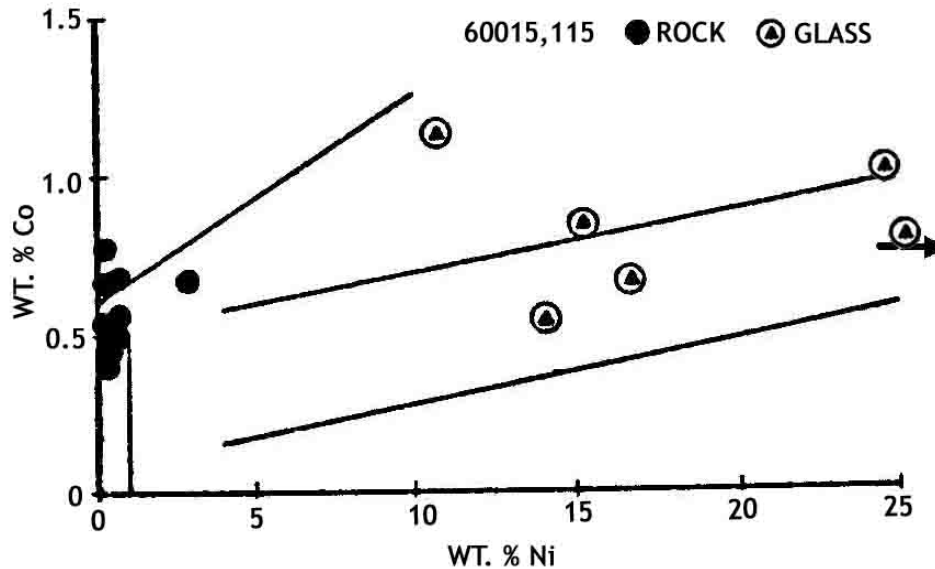


FIGURE 4. Metals; from Hewins and Goldstein (1975a).

**CHEMISTRY:** Chemical studies are listed in Table 1 and summary chemistries of the anorthosite and of the glass coat in Table 2. Representative incompatible element patterns are shown as Figure 5.

For the anorthosite, Laul and Schmitt (1973) note that the REEs are low and identical to 15415 (Fig. 5). Volatile and light elements are very low in abundance (Jovanovic and Reed, 1973; Moore and Lewis, 1976; and others) as are Zr and Hf, with the lowest Zr/Hf of any sample (Garg and Ehmann, 1976). The level of meteoritic contamination, if any, is uncertain because Au, Ir (etc.) have not been measured. Co values are low (1 ppm or less) except for the analysis by Juan et al. (1974) which has 44 ppm Co, and 30 ppm Ni. The low Co contents and the Co/Ni ratios of the metal suggest that most of the anorthosite is uncontaminated. The glass coat was analyzed by Laul and Schmitt (1973) with results in agreement with microprobe data by Dixon and Papike (1975) and Sclar and Bauer (1974). Although similar to Apollo 16 soils, subtle chemical differences exist e.g. lower  $\text{TiO}_2$  (Laul and Schmitt, 1973). The Ni/Au/Ir ratios suggest that the glass was created by the impact of an iron meteorite.

**STABLE ISOTOPES:** Clayton et al. (1973) reported  $\delta\text{O}^{18}$  values of 5.67 for the anorthosite plagioclase and 5.68 for the glass coat, typical lunar values.

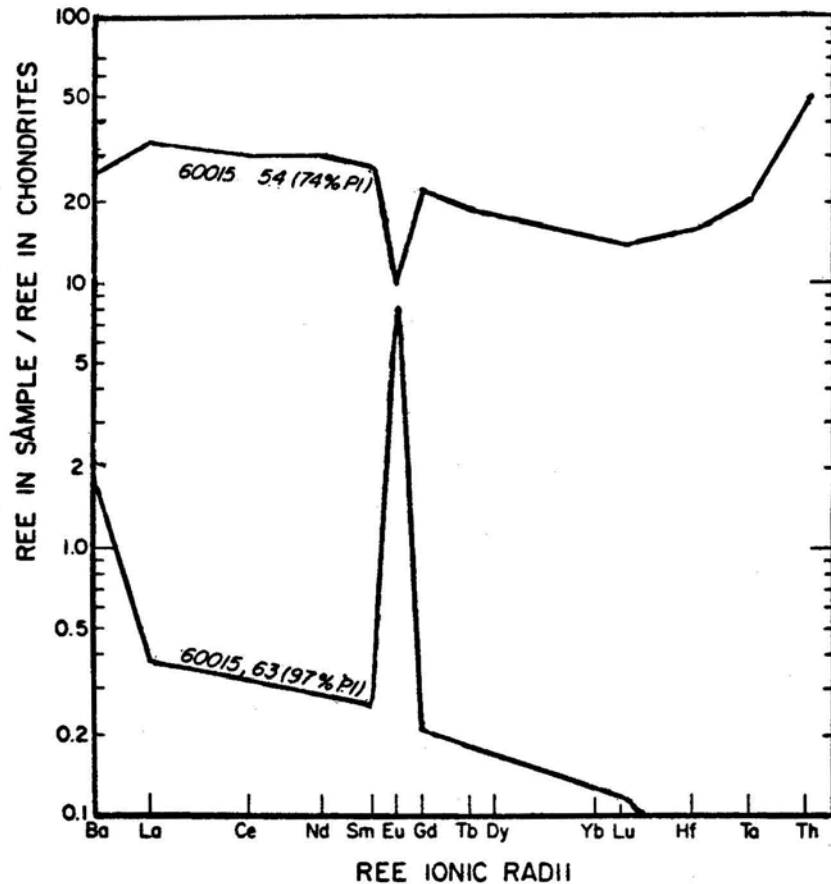


FIGURE 5. Rare earths; from Laul and Schmitt (1973).

RADIOGENIC ISOTOPES AND GEOCHRONOLOGY: Rb-Sr data are summarized in Table 3. The low measured  $^{87}\text{Sr}/^{86}\text{Sr}$  give calculated ratios at 4.6 b.y. close to BABI. Nyquist et al. (1975) calculate an isochron age from two whole rock samples as  $3.8 \pm 1.7$  b.y. but because of the large error do not attribute significance to it. Two plagioclase clasts from the glassy rind have  $^{87}\text{Sr}/^{86}\text{Sr}$  at 4.6 b.y., even lower than the anorthosite (Nunes et al., 1974).

Ar-Ar ages of  $3.5 \pm 0.05$  b.y. (Fig. 6) (Schaeffer and Husain 1974) and  $3.54 \pm 0.05$  b.y. (Fig. 7) (Phinney et al., 1975) demonstrate that the shock melting of the anorthosite was later than the  $\sim 4.0$  b.y. cataclysm. These ages may just be lower limits but a good plateau was obtained by Schaeffer and Husain (1974).

The U-Th-Pb data (Nunes et al., 1973, 1974) indicate an enrichment in Pb at 3.57 b.y. (2-stage model) or 3.8 b.y. (3-stage model). The Pb introduction was presumably contemporaneous with the shock-melting event. These theoretically valid model-dependent ages may not be as precise as first believed because up to 3% of the Pb may be contamination (Nunes et al., 1974).

TABLE 1. Chemical studies of 60015.

<u>Reference</u>	<u>Split #</u>	<u>Description</u>	<u>Elements analyzed</u>
S.R. Taylor <u>et al.</u> (1973)	,64	anorthosite	majors, REEs, other trace
Janghorbani <u>et al.</u> (1973)	,65	"	majors
Laul and Schmitt (1973)	,6	"	majors, REEs, other trace
"	,54	glass coat	"
Juan <u>et al.</u> (1974)	,67	anorthosite	majors, some trace
Nunes <u>et al.</u> (1973)	,50	"	U, Th, Pb
Ehmann and Chyj (1974)	,65B	"	Zr, Hf
Garg and Ehmann (1976)	,65A	"	Eu, Zr, Fe, Cr, Sc, Co, Hf
Miller <u>et al.</u> (1974)	,65B	"	Fe, Cr, Sc, Co, Eu
Schaeffer and Husain (1974)	,22 ,69	"	K, Ca
Jovanovic and Reed (1973)	,60	"	F, Cl, Br, I, Te, U, P <sub>2</sub> O <sub>5</sub>
Moore <u>et al.</u> (1973)	,61	"	C
"	,53	glass coat	C
Cripe and Moore (1974)	,61	anorthosite	S
"	,53	glass coat	S
Moore and Lewis (1976)	,61	anorthosite	N
"	,53	glass coat	N
Phinney <u>et al.</u> (1975)	?	"	K, Ca
Nyquist <u>et al.</u> (1975)	,50I ,50II	"	Rb, Sr
Papanastassiou and Wasserburg (1976)	,36 ,95	"	Rb, Sr, K
Nunes <u>et al.</u> (1974)	,46	glass coat	Rb, Sr, K, U, Th

RARE GAS/EXPOSURE AGES: Leich and Niemeyer (1975) provide Xe, Ar and Kr isotopic data and report an <sup>81</sup>Kr-Kr exposure age of  $1.96 \pm 0.08$  m.y., or  $1.93 + 0.08$  m.y. if the trapped xenon in the rock is terrestrial. The latter interpretation of the origin of the trapped xenon is preferred following experiments (Niemeyer and Leich, 1976) which showed much more Ar, Xe and Kr in crushed samples, even though temperatures greater than 1000° were required to release 75% of the trapped Kr and Xe.

Phinney et al. (1975) and Schaeffer and Husain (1974) report Ar isotopic data and calculate <sup>38</sup>Ar-Ca exposure ages of  $3 \pm 1$  m.y., and  $4.6 \pm 0.6$  and  $6.1 \pm 0.5$  m.y. respectively. These are significantly higher than the <sup>81</sup>Kr-Kr age which Leich and Niemeyer (1975) consider more reliable.

MICROCRATERS AND TRACKS: Several studies of microcraters on the glass surface of 60015 have been made. The surface is in production, not equilibrium. Size-frequency data is provided by Neukum et al. (1973), Horz et al. (1974), Fechtig et al. (1974), Mandeville (1976), and Hartung et al. (1977) (Fig. 8). Neukum et al. (1973), Nagel et al. (1975), and Mandeville (1976) provide measurements of pit characters. Flavill et al. (1978) discuss some of the craters as being of secondary or tertiary origin rather than of direct micrometeoroid origin, and Hartung et al. (1977) note that the data do not specify

that there was a variation of the meteoroid flux with time. Carey and McDonnell (1976) find no evidence for the build-up of sputtered weld material on the surface. Storzer et al. (1973) plot the solar flare track density against depth, as deduced from cratering statistics.

TABLE 2. Summary chemistries of anorthosite and glass coat in 60015.

	<u>Anorthosite</u>	<u>Glass Coat</u>
SiO <sub>2</sub>	44	44
TiO <sub>2</sub>	0.02	0.4
Al <sub>2</sub> O <sub>3</sub>	36	27
Cr <sub>2</sub> O <sub>3</sub>	<0.01	0.1
FeO	0.35	5
MnO	<0.01	0.05
MgO	~0.3	6 - 9
CaO	19	15
Na <sub>2</sub> O	0.4	~0.45
K <sub>2</sub> O	<0.01	0.08
P <sub>2</sub> O <sub>5</sub>	0.01	
Sr	178	157
La	0.13	11
Lu	0.003	0.49
Rb	?	1.9
Sc	0.6	5.8
Ni		900
Co	1	42
Ir ppb		23
Au ppb		8
C	20	59
N	23	50
S	27	890
Zn		
Cu	2	

Oxides in wt%, others in ppm except as noted.

**PHYSICAL PROPERTIES:** The remanent magnetism characteristics of the anorthosite have been studied by Runcorn's group (Collinson et al., 1973; Stephensen et al., 1974, 1975) using the anhysteretic remanent magnetization method (ARM). The rock does not appear to possess a measurable hard NRM, although grains capable of holding such an NRM are present. This is probably due to the extremely low iron content. The initial susceptibility and the saturation remanence are very low. Weeks (1973) studied electron paramagnetic resonance characteristics and noted that Fe<sup>3+</sup> and Ti<sup>3+</sup> are higher than in several other Apollo 16 rocks.

TABLE 3. Summary of Rb-Sr data\* for 60015.

Sample	Description	Rb/Sr	$^{87}\text{Sr}/^{86}\text{Sr}$ Measured	$^{87}\text{Sr}/^{86}\text{Sr}$ Calc. at 4.6 b.y.	Reference
,50 I	Anorthosite	0.00165	0.69934 $\pm$ 4	0.69902	Nyquist <i>et al.</i> 1975
,50 II	"	0.00044	0.69915 $\pm$ 5	0.69907	"
,50	"	0.00073	0.69904 $\pm$ 6	0.69890	Nunes <i>et al.</i> 1974
,36	"	0.00016	0.69903 $\pm$ 3	0.69900	Papanastassiou and Wasserburg 1976
,95	"	0.00067	0.69908 $\pm$ 4	0.69895	"
,46	Plag. in glass	0.00083	0.69900 $\pm$ 7	0.69884	Nunes <i>et al.</i> 1974
,46	"	0.00044	0.69887 $\pm$ 3	0.69878	"
,46	Glass coat	0.01218	0.70120 $\pm$ 6	0.69888	"

\*Not corrected for interlaboratory bias.

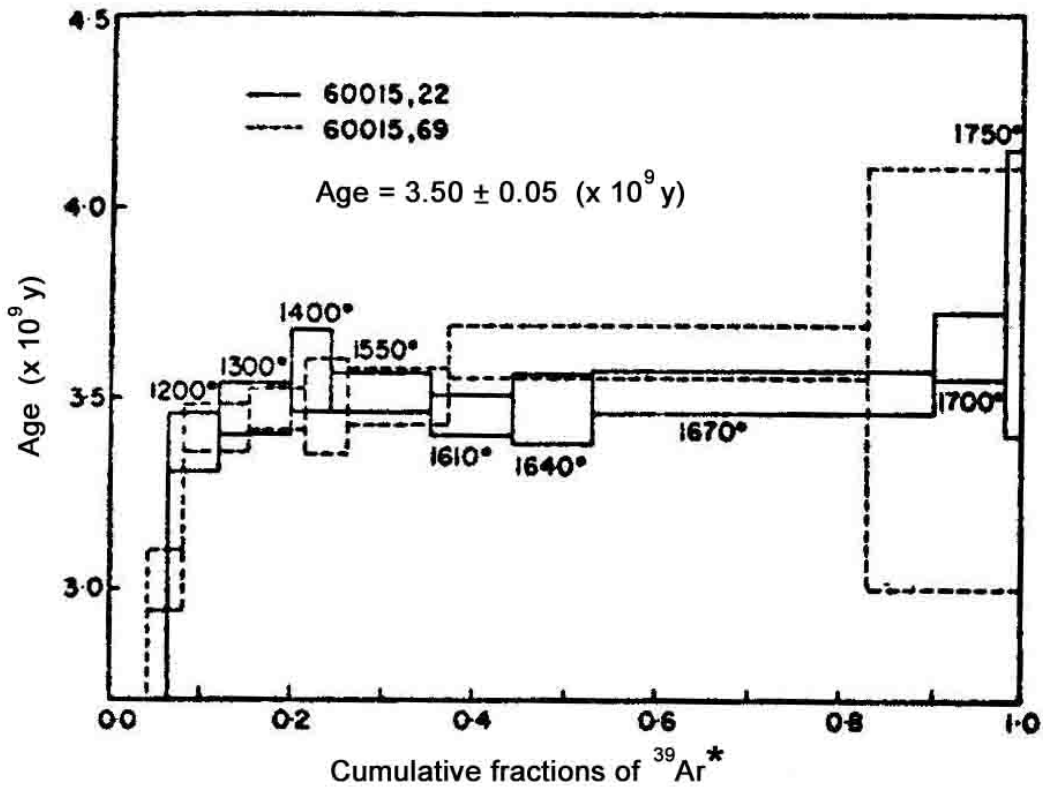


FIGURE 6. Ar release; from Schaeffer and Husain (1974).

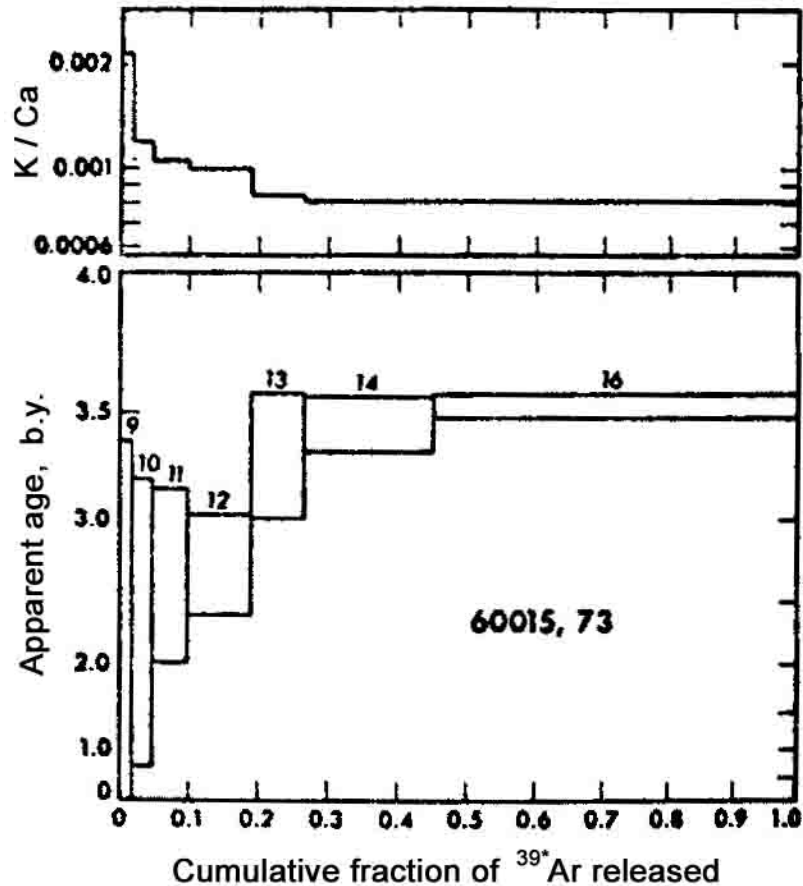


FIGURE 7. Ar release; from Phinney et al. (1975).

P and S wave velocities of the anorthosite from 0.5 to 7 kb are reported in Chung (1978) (Table 4, Fig.9). Herminghaus and Berckhmer (1974) measured Q with ultrasonic absorption measurements at  $10^{-4}$  torr and  $+20^{\circ}\text{C}$  to  $-180^{\circ}\text{C}$ . Q is quite low, independent of T, and at  $20^{\circ}\text{C}$  only 20% higher than at atmospheric pressure. The measurements suggest that the anorthosite has a high microcrack density.

Dielectric constants and losses for the anorthosite are presented in Chung and Westphal (1973) (Fig.10).

Mandeville and Dollfus (1977) determined polarimetric properties of surface portions of 60015, one cratered and dust-free, others cratered and dust-covered.

PROCESSING AND SUBDIVISIONS: In 1972, 60015 was sawn into 5 main pieces (Fig.11). The large pieces ,1 and ,2 are preserved intact and ,3 was subdivided into 3 pieces for display purposes. All allocations are from the two slabs produced during sawing. The main subdivision of these slabs and the locations of the splits are shown in Figures 12 and 13. Several subsequent splits and renumbering of returned/consumed samples are not shown.

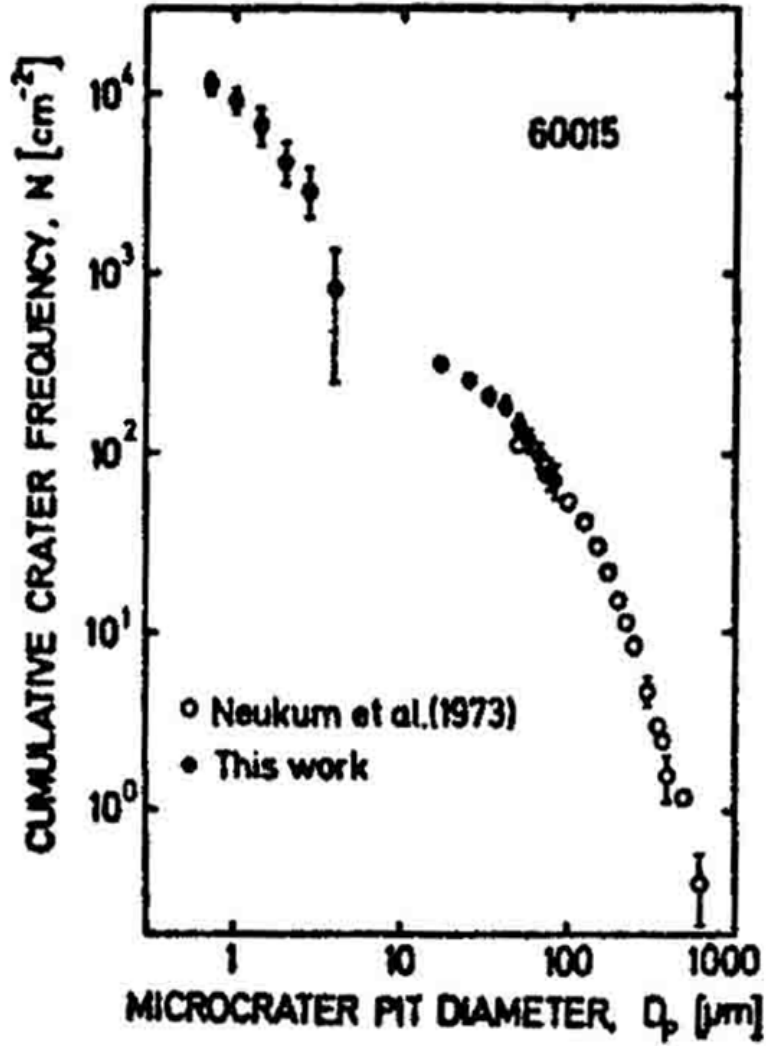


FIGURE 8. Microcraters; from Fechtig et al. (1974).

TABLE 4. Elastic wave velocities of anorthosite in 60015.

	Confining pressure (Kb)									
	0.5	1.0	1.5	2	3	4	5	6	7	10*
P Km/s	5.5	6.0	6.27	6.52	6.75	6.86	6.90	6.94	6.97	7.02
S Km/s	2.6	2.9	3.21	3.40	3.58	3.68	3.74	3.86	3.88	3.91

\*Estimated by linear extrapolation. Reference: Chung (1973)

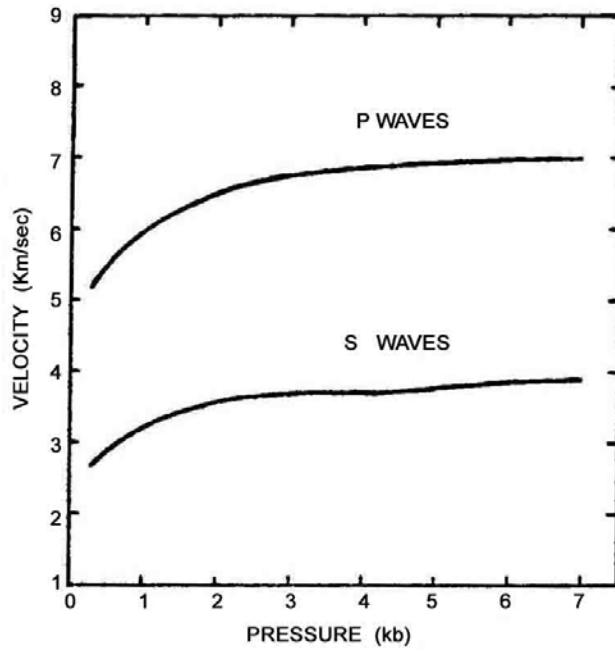


FIGURE 9. from Chung (1973).

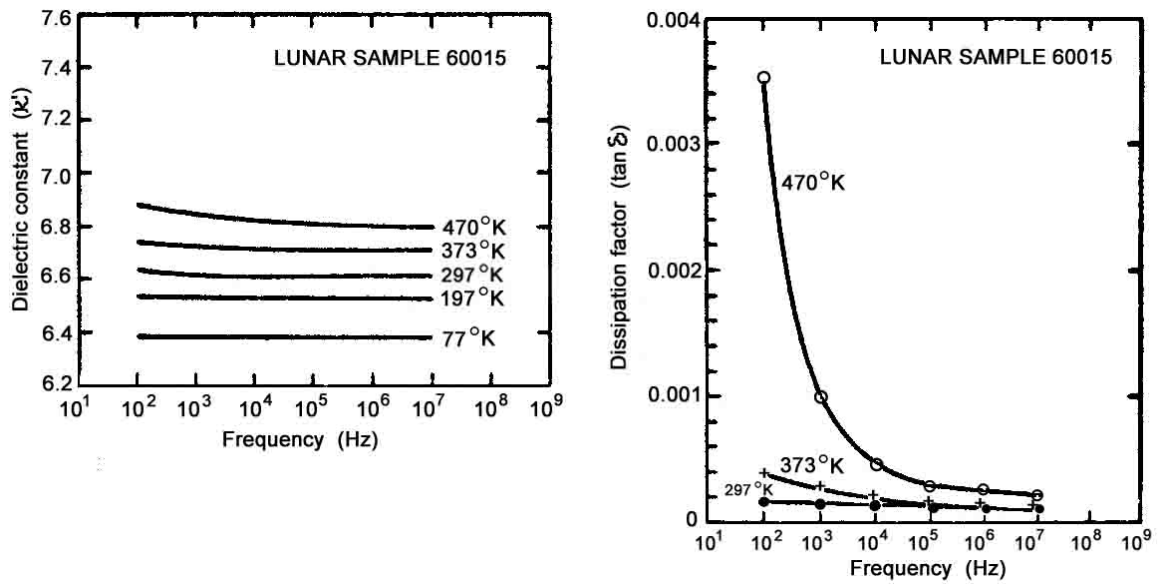


FIGURE 10. Dielectric properties; from Chung and Westphal (1973).

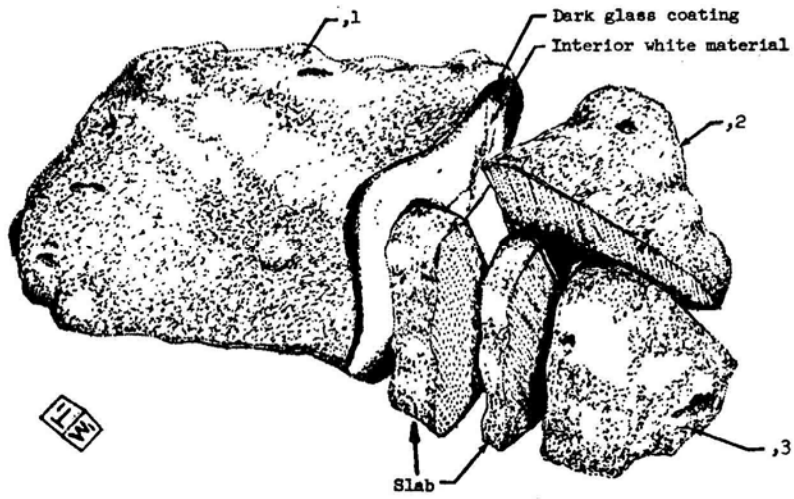


FIGURE 11.

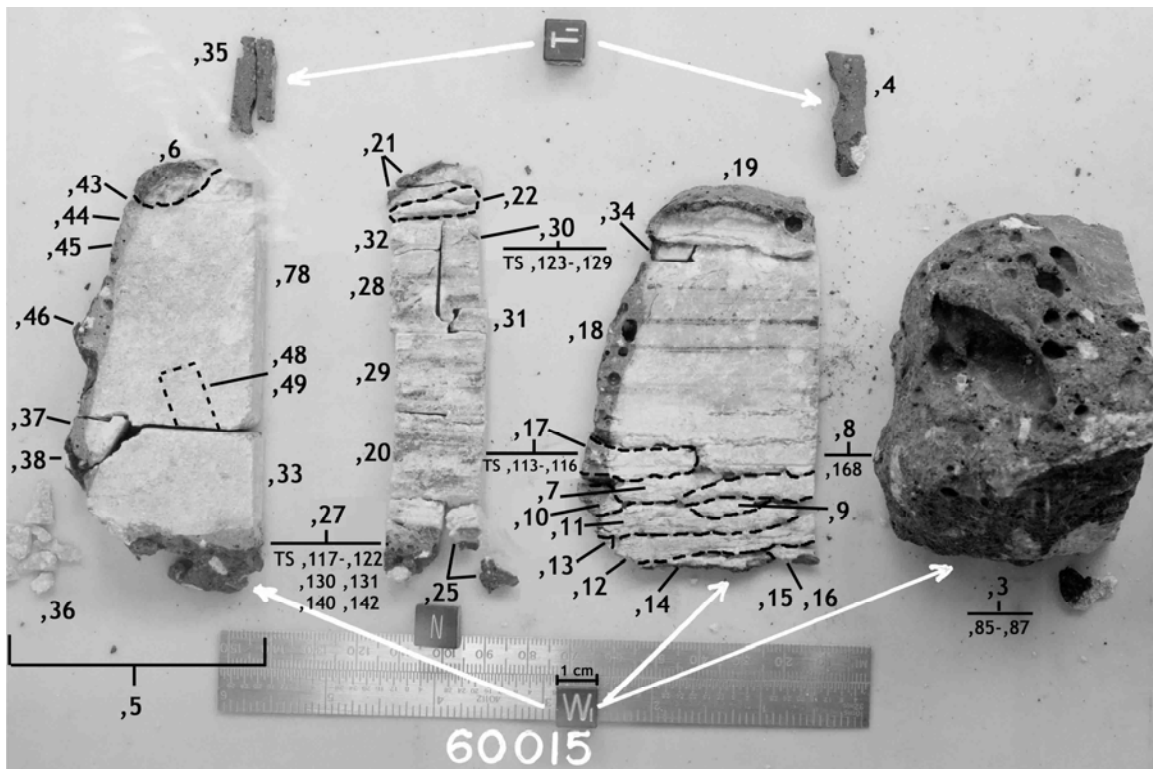


FIGURE 12. S-72-54203.

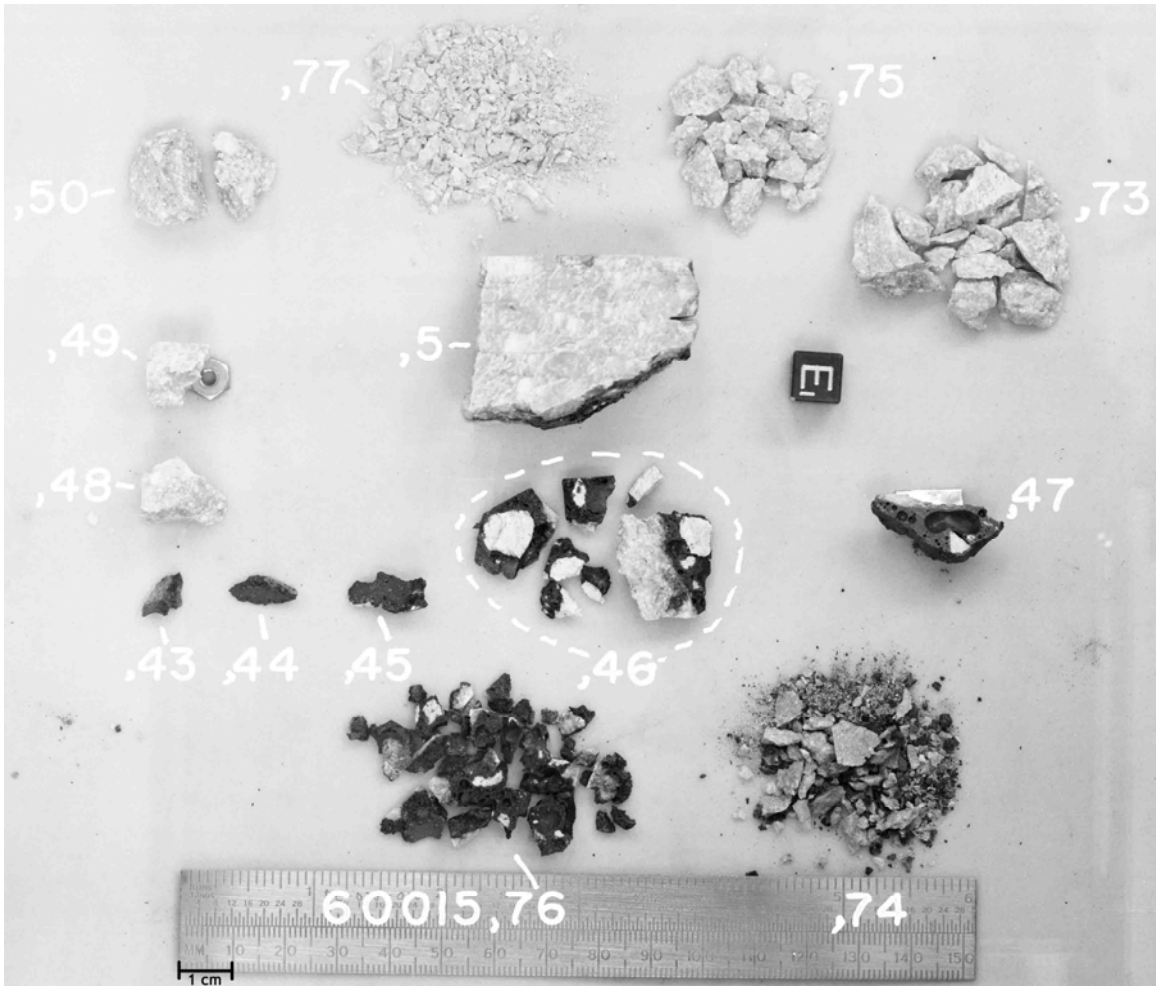


FIGURE 13. S-72-55505.